

Contact Angle Hysteresis in a Solid-on-Solid Model

P. Collet,¹ J. De Coninck,² and F. Dunlop¹

Received June 22, 1993

The hysteresis of the contact angle of a sessile drop on top of a disordered substrate is studied within a two-dimensional solid-on-solid model using Monte Carlo dynamics. Numerical and analytical evidence is given to show that there is always a hysteresis even for small densities of impurities.

KEY WORDS: Hysteresis; solid-on-solid model; Monte Carlo dynamics.

1. INTRODUCTION

The phenomenon of contact angle hysteresis has been considerably studied from an experimental point of view.⁽¹⁻³⁾ It is now generally accepted that this property is due to chemical heterogeneities on top of the substrate or due to the roughness of the substrate.⁽⁴⁻⁶⁾ From a microscopic point of view, just a few results have been obtained so far, neglecting the associated thermal fluctuations.^(7,8) There are, however, some aspects of the problem which remain unclear, such as the fact that even for a small density of impurities on top of the substrate, there would always be a hysteresis in the absence of external field (e.g., the gravitational field). This seems in contradiction with the natural idea that the thermal fluctuations of the interface should wash out small heterogeneities at the molecular scale.

In a previous paper on a two-dimensional microscopic model⁽⁹⁾ we studied this hysteresis neglecting all thermal fluctuations other than those of the contact point between the interface and the substrate, and concluded that hysteresis is present at arbitrarily small disorder. This left open the question as to whether fluctuations of the interface itself would pull the contact point out of traps made by the disorder, and thus remove

¹ Centre de Physique Théorique (CNRS Laboratory UPR 14) Ecole Polytechnique, F-91128 Palaiseau Cedex, France. dunlop@orphee.polytechnique.fr.

² Université de Mons-Hainaut, 7000 Mons, Belgium.

hysteresis when the disorder was weak and the temperature high enough. This motivates the present work, where we keep all the dynamical degrees of freedom of the interface, still in two dimensions.

We use a solid-on-solid approximation of the interface and study the corresponding Monte Carlo dynamics. Section 2 presents the model and Section 3 gives the main results of our numerical simulations. Analytical estimates which confirm our numerical results are presented in Section 4. Some discussion is given in a concluding section.

2. THE RSOS MODEL AND MONTE CARLO DYNAMICS

The advancing edge of our two-dimensional drop is represented by vertical columns describing the height h_i of the profile above a flat substrate, as indicated in Fig. 1. The index i runs from 0 up to a variable point l_t , where the interface meets the substrate, so that $h_i > 0$ for $i = 0, \dots, l_t - 1$ and $h_{l_t} = 0$. The length l_t will be called the *spreading length*. Since we want to study the contact angle, we consider configurations with a fixed value for h_0 , which should be taken to infinity in the thermodynamic limit. The height difference $h_{i+1} - h_i$ is allowed to take values $-1, 0$, or 1 , which corresponds to the so-called RSOS model (restricted-solid-on-solid model).

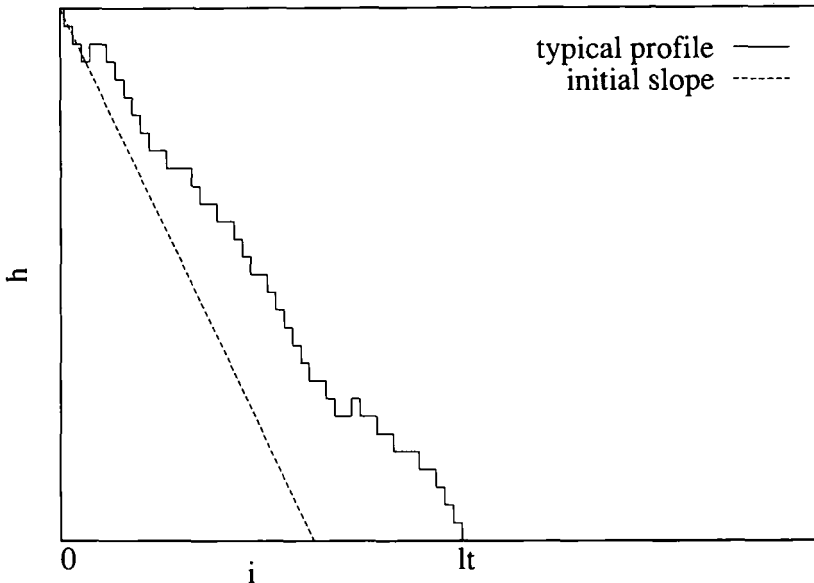


Fig. 1. RSOS configuration for an advancing interface.

The energetic cost of a configuration with an interface of projected length l (the spreading length) is defined according to

$$E_{\xi}(h_0, h_1, \dots, h_{l-1}) = J \sum_{i=0}^{l-1} (1 + |h_{i+1} - h_i|) - \mu l + \sum_{i=0}^{l-1} \xi_i \quad (1)$$

where μ is the difference between the wall free energies with and without the spreading phase, and the quenched random variables ξ_i represent the disorder, i.e., the local variation of the wettability due to impurities or defects compared to that of an ideal substrate. For the numerical simulations presented in the next section, the random variables ξ_i were taken independent and uniformly distributed on an interval $[-b, b]$. More generally the ξ_i will be assumed to be distributed according to a translation-invariant Gibbs state with short-range correlations, zero average, and variance proportional to b^2 . The parameters J , μ , and b are taken as dimensionless multiples of kT , so that the temperature will not appear explicitly in the following:

The partition function

$$Z_{\xi, h_0} = \sum_{l=h_0}^{\infty} \sum_{h_1, \dots, h_{l-1}} \exp[-E_{\xi}(h_0, h_1, \dots, h_{l-1})]$$

is finite almost surely with respect to ξ if and only if

$$\mu < J - \log(1 + 2e^{-J}) \quad (2)$$

which defines the partial wetting regime where contact angles will be strictly positive and spreading lengths proportional to h_0 (see ref. 10 for results in the case of a pure substrate). The equilibrium probability of a configuration is the finite-volume Gibbs measure

$$\Pr_{\xi}(h_1, \dots, h_{l-1}, l) = \frac{1}{Z_{\xi, h_0}} \exp[-E_{\xi}(h_0, h_1, \dots, h_{l-1})]$$

It will be convenient to use the following equivalent representation: given a positive integer h_0 , the configuration space is defined as the set of $\mathbf{h} = \{h_i\}_{i=1}^{\infty}$ such that:

1. $\forall i \geq 0, h_{i+1} - h_i \in \{-1, 0, 1\}$.
2. $\forall i \geq 0, h_i = 0 \Rightarrow h_{i+1} = 0$.
3. $\max\{i | h_i > 0\} < \infty$.

The energy as defined in (1) above can then be written as

$$E_{\xi}(\mathbf{h}) = \sum_{i=0}^{\infty} (J |h_{i+1} - h_i| + (J - \mu + \xi_i)(1 - \delta_{h_i,0})) \quad (3)$$

and the partition function

$$Z_{\xi, h_0} = \sum_{\mathbf{h}} \exp[-E_{\xi}(\mathbf{h})]$$

where the sum is over the configuration space just defined with a given value of h_0 .

Let us now define the dynamics, which is a discrete-time dynamics whereby at each time step we let evolve either the h_i with i odd or the h_i with i even. Letting $\mathbf{h} = (\mathbf{h}^o, \mathbf{h}^e)$, with

$$\mathbf{h}^o = \{h_{2j+1}\}_{j=0}^{\infty}, \quad \mathbf{h}^e = \{h_{2j}\}_{j=0}^{\infty}$$

we take the transition probabilities as follows:

$$\begin{aligned} \Pr_{\xi}((\mathbf{h}^o, \mathbf{h}^e) \rightarrow (\mathbf{h}'^o, \mathbf{h}^e)) &= \frac{1}{2} \frac{\exp[-E_{\xi}(\mathbf{h}'^o, \mathbf{h}^e)]}{\sum_{\mathbf{h}''^o} \exp[-E_{\xi}(\mathbf{h}''^o, \mathbf{h}^e)]} \\ \Pr_{\xi}((\mathbf{h}^o, \mathbf{h}^e) \rightarrow (\mathbf{h}^o, \mathbf{h}'^e)) &= \frac{1}{2} \frac{\exp[-E_{\xi}(\mathbf{h}^o, \mathbf{h}'^e)]}{\sum_{\mathbf{h}''^e} \exp[-E_{\xi}(\mathbf{h}^o, \mathbf{h}''^e)]} \end{aligned} \quad (4)$$

where $\mathbf{h}'^o \neq \mathbf{h}^o$ and $\mathbf{h}'^e \neq \mathbf{h}^e$, and where the factors 1/2 correspond to the probability of either the odd sites or the even sites being updated. The dynamics thus defined satisfies the detailed balance condition and is irreducible, which implies that the time averages will converge to the equilibrium Gibbs measure, starting from any initial configuration.

A simple argument, following the lines of proving a Wulff construction, shows that the equilibrium contact angle θ_c , which in practice may not be reached within observation times, does obey Young's equation for the averaged substrate,

$$\cos \theta_c \sigma(\theta_c) - \sin \theta_c \sigma'(\theta_c) = \mu \quad (5)$$

where $\sigma(\theta)$ is the surface (in fact line) tension, and $\sigma'(\theta)$ its derivative with respect to θ . For one-dimensional SOS models, $\sigma(\theta)$ can be computed explicitly⁽¹¹⁾ and the result in the present case reads

$$\sigma(\theta) = J \cos \theta + c_{\theta} \sin \theta - \cos \theta \log(1 + e^{-J+c_{\theta}} + e^{-J-c_{\theta}}) \quad (6)$$

where c_θ is the solution of

$$\tan \theta = \frac{e^{-J+c_\theta} - e^{-J-c_\theta}}{1 + e^{-J+c_\theta} + e^{-J-c_\theta}} \quad (7)$$

Young's equation has a solution $\theta_c > 0$ when (2) is satisfied, and the equilibrium contact angle thus defined satisfies

$$\tan^2 \theta_c = (1 - e^{-J+\mu})^2 - 4e^{-4J+2\mu} \quad (8)$$

One may be interested in the variation of the equilibrium length $\langle l \rangle_\xi$ from sample to sample. This can be obtained from the free energy conditioned by given values of l , near the value l_c corresponding to the averaged substrate:

$$F_l - F_{l_c} = \frac{\sin^3 \theta}{2(\sigma + \sigma'')} \frac{(l_c - l)^2}{h_0} + \sum_{i=1}^{l_c} \xi_i + \mathcal{O}(\log l)$$

The term coming from the disorder is almost surely of order $b |l_c - l|^{1/2}$, which dominates as long as

$$|l - l_c| \ll h_0^{2/3} \approx l_c^{2/3}$$

The most likely value of l will therefore differ from l_c almost surely by order $l_c^{2/3}$.

3. NUMERICAL RESULTS

We consider initial configurations which are straight interfaces with various contact angles such as shown in Fig. 1. For the ideal substrate ($\xi_i = 0$ for all i), the interface relaxes in a time of the order of h_0^2 Monte Carlo steps per site to the equilibrium profile, starting from any initial angle. However, if the amplitude b of the disorder is large enough, we observe that the graph of the spreading length l_t as a function of time t presents various plateaux as reproduced in Fig. 2.

When a plateau has a lifetime of order larger than h_0^2 , which corresponds to the experimental time scale, the interface is trapped. The first such trap met by the interface will be the observed angle, which defines an advancing angle or a receding angle depending on the initial conditions.

In order to investigate the uniqueness of the advancing angle in the thermodynamic limit, we have simulated the time evolution of the advancing

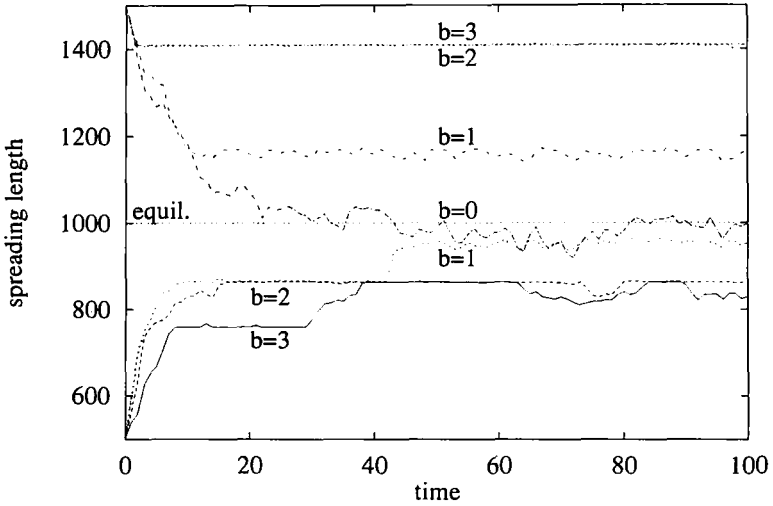


Fig. 2. Spreading length versus time for advancing interfaces with $b=3, 2, 1, 0$ and for receding interfaces with $b=0, 1, 2, 3$, from bottom to top. The maximum time is $(1.25) 10^7$ MC steps/site, the initial length is 500 for the advancing interfaces and 1500 for the receding ones. $J=2$, and μ is chosen such that $t_c = 1000$. The random variables ξ_i take the same values for the eight runs.

edge for several substrates, independently chosen with the same distribution of ξ . In Fig. 3 we reproduce for various values of h_0 the histogram of the variable l obtained by counting how many times l , falls in given intervals, at times greater than twice the pure relaxation time ($t_{\min} = 2t_{\text{relax}} = 10h_0^2$) and less than ten times this time ($t_{\max} = 10t_{\text{relax}} = 50h_0^2$),

$$I(l) = \frac{1}{t_{\max} - t_{\min}} \sum_{t=t_{\min}+1}^{t_{\max}} \left\langle \chi \left(l - \frac{l_0}{40} \leq l_t < l + \frac{l_0}{40} \right) \right\rangle_{\xi}$$

where the brackets indicate an average over a certain number of runs with different realizations of the substrate, and χ is an indicator function.

The initial condition was always $l_0 = h_0$. The results support the conjecture that, in the thermodynamic limit ($h_0 \rightarrow \infty$), the associated distribution of the advancing contact angle reduces to a delta distribution. In other words, on the time scale of the time for relaxation to equilibrium in the pure case, the advancing angle is self-averaging. Its precise value depends on the various parameters in the problem, on the probability distribution of the disorder, and in particular on b . A heuristic discussion of this dependence is given in the next section.

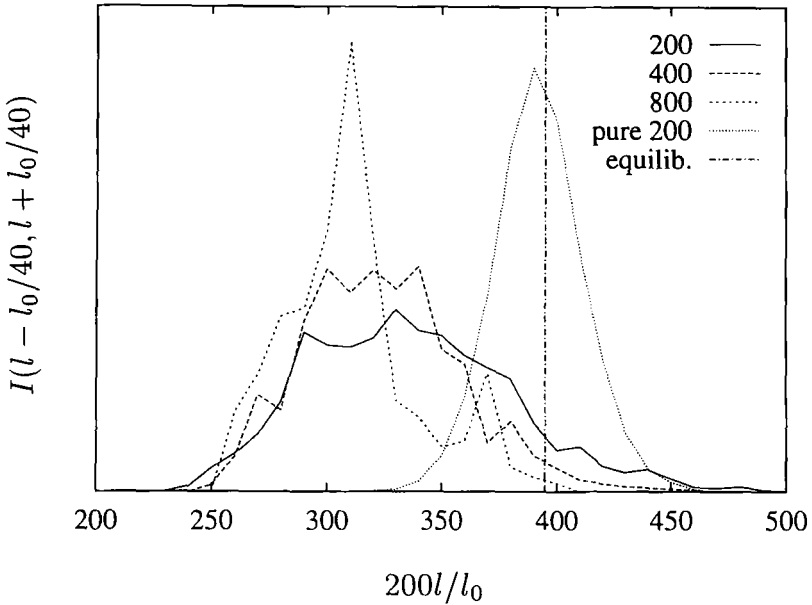


Fig. 3. Histogram of the spreading length for $h_0 = 200, 400, 800$ with disorder $b = 3$, and for $h_0 = 200$ with a pure substrate. $J = 2$, $\mu \simeq 1.26$, giving $l_{eq} \simeq 1.97h_0$. The initial length is $l_0 \simeq h_0$. The histogram is built from times between $10h_0^2$ and $50h_0^2$ measured in MC steps per site, and is averaged over a number of substrates equal to 1000, 320, 48, respectively, when $b = 3$, or over 10 runs in the case of the pure substrate.

4. ANALYTICAL RESULTS

In this section, we assume that the random variables ξ_j are distributed according to a translation-invariant Gibbs state with short-range correlations (denoted by $\langle \cdot \rangle$) and with zero average.

We recall the large-deviation result for one-dimensional Gibbs states with short-range correlations. Let

$$S_n = \sum_{j=0}^{n-1} \xi_j$$

It is well known⁽¹²⁾ that the following limit exists:

$$P(x) = \lim_{n \rightarrow \infty} \frac{1}{n} \log \langle e^{xS_n} \rangle \quad (9)$$

This function is real analytic and we have for $\alpha > 0$

$$\Pr(S_n > n\alpha) \approx e^{-nI(\alpha)}$$

where f is the Legendre transform of P , namely

$$\begin{aligned} x &= f'(\alpha) \\ P(x) &= x\alpha - f(\alpha) \end{aligned} \tag{10}$$

We recall also that P is strictly convex with $P(0) = P'(0) = 0$, f is concave with $f(0) = f'(0) = 0$, and in the above result the symbol \approx means precisely (for $\alpha > 0$)

$$f(\alpha) = - \lim_{n \rightarrow \infty} \frac{1}{n} \log \Pr(S_n > n\alpha)$$

We now consider a given spreading length l_1 corresponding to an angle $\theta > \theta_c$. We compute the variation of free energy when the position is n steps further right, where the contact angle has decreased to $\theta + \delta\theta$ with

$$\delta\theta = - \frac{n \sin^2 \theta}{h_0}$$

If $n \ll h_0$, to the leading order in n , the variation $F_{l_1+n} - F_{l_1}$ of the free energy conditioned by the given values of l reads

$$\begin{aligned} F_{l_1+n} - F_{l_1} &\simeq \frac{h_0}{\sin(\theta + \delta\theta)} \sigma(\theta + \delta\theta) - \frac{h_0}{\sin \theta} \sigma(\theta) - \mu n + \sum_{j=l_1+1}^{l_1+n} \xi_j \\ &\simeq -(\mu - \sigma \cos \theta + \sigma' \sin \theta)n + S_n(l_1) \end{aligned}$$

The event $S_n(l_1) > n\alpha$ will occur almost surely in the thermodynamic limit somewhere on an interval $[l, l + \varepsilon l]$ if we have

$$\Pr(S_n > n\alpha) > (\varepsilon l)^{-1}$$

This implies that, for any $\alpha > 0$, the largest n realized almost surely is given by

$$n \approx \frac{\log l}{f(\alpha)}$$

We then get for the corresponding energy barrier to the right

$$\frac{\alpha - (\mu - \sigma \cos \theta + \sigma' \sin \theta)}{f(\alpha)} \log l$$

The time needed to pass such a barrier is of the order of the exponential of this number and is therefore a power of l , namely l^γ with

$$\gamma = \frac{\alpha - (\mu - \sigma \cos \theta + \sigma' \sin \theta)}{f(\alpha)}$$

We now maximize the number γ with respect to α . We get

$$\frac{d\gamma}{d\alpha} = \frac{f(\alpha) - [\alpha - (\mu - \sigma \cos \theta + \sigma' \sin \theta)] f'(\alpha)}{f(\alpha)^2} = 0$$

which is easier to formulate using the function P and the variable $x = f'(\alpha)$, namely

$$\gamma(\theta) = \frac{1}{x} \quad \text{with} \quad \mu - \sigma \cos \theta + \sigma' \sin \theta = \frac{P(x)}{x} \quad (11)$$

If we now assume

$$\mu - \lim_{x \rightarrow +\infty} \frac{P(x)}{x} < \sigma \cos \theta - \sigma' \sin \theta < \mu \quad (12)$$

then the strict convexity of P with $P'(0)=0$ implies the existence of a unique $x = x(\theta) > 0$ satisfying Eq. (11). Using

$$\sigma \cos \theta - \sigma' \sin \theta = J - \log(1 + e^{-J+c_\theta} + e^{-J-c_\theta})$$

with c_θ given by (7), we see that this expression is a monotone decreasing function of θ . The second inequality in (12) is just $\theta > \theta_c$. The first inequality means that θ is less than the equilibrium angle corresponding to a substrate where ξ would be a constant equal to its maximum allowed value. One can see also that $x(\theta)$ is monotone increasing in θ and $x(\theta) \searrow 0$ as $\theta \searrow \theta_c$, so that $\gamma(\theta) \nearrow \infty$ as $\theta \searrow \theta_c$.

When the exponent $\gamma(\theta)$ is less than two, it will be hidden by the exponent, equal to two, for relaxation of the interface itself with both ends pinned. Therefore we propose a definition of the advancing angle, physically the angle where the interface is stuck, in the present context, as the angle at which $\gamma(\theta) = 2$, i.e., θ_a such that

$$\sigma \cos \theta_a - \sigma' \sin \theta_a = \mu - 2P(1/2) \quad (13)$$

or

$$\tan^2 \theta_a = (1 - e^{-J + \mu - 2P(1/2)})^2 - 4e^{-4J + 2\mu - 2P(1/2)} \quad (14)$$

Let us now consider specific cases. First, independent impurities distributed as in ref. 9:

$$\begin{aligned}\xi_i &= -db && \text{with probability } 1-d \\ \xi_i &= b-db && \text{with probability } d\end{aligned}$$

We find

$$\begin{aligned}P(x) &= -dbx + \log[1 + d(e^{bx} - 1)] \\ f(\alpha) &= \left(d + \frac{\alpha}{b}\right) \log\left(1 + \frac{\alpha}{bd}\right) + \left(1 - d - \frac{\alpha}{b}\right) \log\left(\frac{1 - d - \alpha/b}{1 - d}\right)\end{aligned}$$

and

$$\sigma \cos \theta_a - \sigma' \sin \theta_a = \mu + db - 2 \log[1 + d(e^{b/2} - 1)] \quad (15)$$

Another case is the distribution of disorder chosen in the numerical simulations presented in Section 3, namely ξ_i independent uniformly distributed in $[-b, b]$, for which we find

$$\begin{aligned}P(x) &= \log \frac{\sinh(xb)}{xb} \\ \sigma \cos \theta_a - \sigma' \sin \theta_a &= \mu - 2 \log \left[\frac{2}{b} \sinh \left(\frac{b}{2} \right) \right] \equiv \mu_a(b)\end{aligned} \quad (16)$$

or

$$\tan^2 \theta_a = (1 - e^{-J + \mu_a(b)})^2 - 4e^{-4J + 2\mu_a(b)} \quad (17)$$

Applying this formula to the set of parameters corresponding to Fig. 3 gives

$$200l_a/l_0 \simeq 263 \quad (18)$$

Comparing with Fig. 3, we observe that the peak of the histogram becomes narrower and shifted to the left as $h_0 = 200, 400, 800$ increases. It is clear also that finite-size corrections and broadening are much more pronounced in the disordered case than in the ordered case.

5. DISCUSSION

We have obtained simple analytical formulas for the contact angle hysteresis in two dimensions, in the framework of solid-on-solid models

with disorder of arbitrary amplitude. These formulas also apply to isotropic interfaces, i.e., for fluids. The amplitude of the hysteresis, as measured by comparing the advancing angle to the ultimate equilibrium angle, is then given by

$$\cos \theta_e - \cos \theta_a = \frac{2}{\sigma} P\left(\frac{1}{2}\right) \tag{19}$$

where, for uncorrelated disorder,

$$P\left(\frac{1}{2}\right) = \log \langle e^{\xi - \langle \xi \rangle} \rangle$$

The corresponding graphs are given in Fig. 4 and reveal that impurities distributed uniformly in an interval $[-b, b]$, covering all sites of the substrate, induce a larger hysteresis effect than simple impurities of fixed magnitude b scattered with a density d on the substrate, whatever the density d .

The advancing contact angle is associated with a time scale of order l^2 . Our study also provides an estimate of the time needed to reach the true

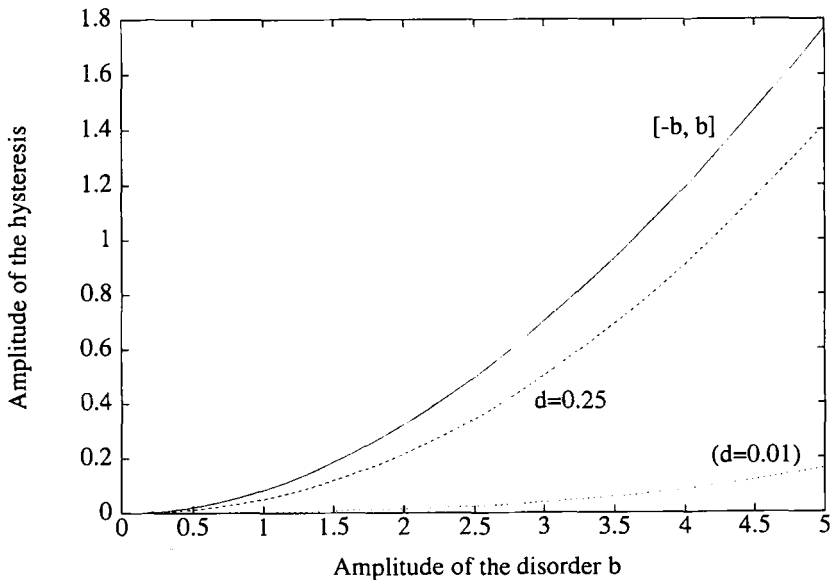


Fig. 4. The amplitude of the contact angle hysteresis $\cos \theta_e - \cos \theta_a$ as a function of the amplitude of the disorder b for a given interfacial tension $\sigma = 1$, showing the case of disorder distribution uniform in $[-b, b]$ and the case of impurities of fixed amplitude b scattered at random with density $d = 0.25$ and $d = 0.01$.

equilibrium in presence of disorder. Let us first remark that the time scale $T(\theta) \approx l^{n(\theta)}$, which is l^2 for $\theta = \theta_c$, diverges as $\theta \searrow \theta_c$:

$$\gamma(\theta) \approx (\cos \theta_c - \cos \theta)^{-1} \quad \text{as } \theta \searrow \theta_c$$

When $l_c - l$ is of order smaller than l_c , the analysis takes a slightly different form: we consider intervals of length $l_c - l$ centered at l and look for large deviations of the disorder, $S_n > n\alpha$, in the given intervals. The width n of the trap is now restricted to $n < l_c - l$. Our estimate for $\gamma(\theta)$ corresponds to a choice $n \approx \log(l_c - l)/f(\alpha)$, and a choice of α such that

$$f(\alpha) \approx \alpha^2 \approx (\theta - \theta_c)^2 \approx \left(\frac{l_c - l}{l_c}\right)^2 \quad \text{as } \theta \searrow \theta_c$$

The condition $n < l_c - l$ then requires

$$l_c - l > l_c^{2/3} (\log l_c)^{1/3}$$

The time to reach $l = l_c - l_c^{2/3} (\log l_c)^{1/3}$ is then found to behave as $\exp[\mathcal{O}(l_c^{1/3} (\log l_c)^{2/3})]$.

The phenomenon of contact angle hysteresis takes place normally in the partial wetting regime, away from the wetting transition, whose order, first or second, perhaps modified by the disorder, is not important here. The results of the present paper are even qualitatively the same as those given for a simplified model⁽⁹⁾ where only the dynamics of the contact point was studied. This shows that the fluctuations of the other degrees of freedom do not play an important role in this hysteresis, away from the wetting transition. We expect, on the other hand, that the dimension definitely plays a role in the process of contact angle hysteresis.

ACKNOWLEDGMENTS

The authors acknowledge support from CNRS, FNRS, and CGRI, which made this collaboration possible. This work also presents research results of the Belgian Program on Interuniversity Poles of Attraction initiated by the Belgian State, Prime Minister's Office, Science Policy Programming. The scientific responsibility is assumed by the authors.

REFERENCES

1. A. W. Adamson, *Physical Chemistry of Surfaces* (Wiley, New York, 1990).
2. A. W. Neumann, Contact angles and their temperature dependence: Thermodynamic status, measurement, interpretation and application, *Adv. Colloid Interface Sci.* **4**:105-191 (1974).

3. L. S. Penn and B. Miller, A study of the primary cause of contact angle hysteresis on some polymeric solids, *J. Colloid Interface Sci.* **78**:238–241 (1980).
4. P. G. de Gennes, Wetting: Statics and dynamics, *Rev. Mod. Phys.* **57**:827–863 (1985).
5. J. F. Joanny and P. G. de Gennes, A model for contact angle hysteresis, *J. Chem. Phys.* **81**:552–562 (1984).
6. L. Léger and J. F. Joanny, Liquid spreading, *Rep. Prog. Phys.* **1992**:431–486.
7. Y. Pomeau and J. Vannimenus, Contact angle on heterogeneous surfaces: Weak heterogeneities, *J. Colloid Interface Sci.* **104**:477 (1985).
8. M. O. Robbins and J. F. Joanny, Contact angle hysteresis on random surfaces, *Europhys. Lett.* **3**:729–735 (1987).
9. P. Collet, J. De Coninck, and F. Dunlop, Dynamics of wetting with a disordered substrate: The contact angle hysteresis, *Europhys. Lett.* **22**:645–650 (1993).
10. J. De Coninck, F. Dunlop, and F. Menu, Spreading of a solid-on-solid drop, *Phys. Rev. E* **47**:1820–1823 (1993).
11. J. De Coninck, F. Dunlop, and F. Menu, Exact results for a meniscus within an SOS-type approximation, *J. Stat. Phys.* **61**:1121–1139 (1990).
12. D. Ruelle, *Thermodynamic Formalism* (Addison-Wesley, Reading, Massachusetts, 1978).